AGU PUBLICATIONS

Geochemistry, Geophysics, Geosystems

RESEARCH ARTICLE
10.1002/2015GC006017

Special Section:
The Lithosphere-asthenosphere System

Toward the reconciliation of seismological and petrological perspectives on oceanic lithosphere heterogeneity

B. L. N. Kennett[1] and T. Furumura[2]

[1]Research School of Earth Sciences, Australian National University, Canberra, Australian Capital Territory, Australia, [2]Earthquake Research Institute, University of Tokyo, Tokyo, Japan

Abstract The character of the high-frequency seismic phases *Po* and *So*, observed after propagation for long distances in the oceanic lithosphere, requires the presence of scattering from complex structure in 3-D. Current models use stochastic representations of seismic structure in the oceanic lithosphere. The observations are compatible with quasi-laminate features with horizontal correlation length around 10 km and vertical correlation length 0.5 km, with a uniform level of about 2% variation through the full thickness of the lithosphere. Such structures are difficult to explain with petrological models, which would favor stronger heterogeneity at the base of the lithosphere associated with underplating from frozen melts. Petrological evidence mostly points to smaller-scale features than suggested by seismology. The models from the different fields have been derived independently, with various levels of simplification. Fortunately, it is possible to gently modify the seismological model toward stronger basal heterogeneity, but there remains a need for some quasi-laminate structure throughout the mantle component of the oceanic lithosphere. The new models help to bridge the gulf between the different viewpoints, but ambiguities remain.

Key Points:
- A unified model for fine-scale heterogeneity in the oceanic lithosphere
- Stronger heterogeneity near base of lithosphere links to changes in radial anisotropy
- Expected age dependence in nature of fine-scale heterogeneity

Correspondence to:
B. L. N. Kennett,
brian.kennett@anu.edu.au

Citation:
Kennett, B. L. N., and T. Furumura (2015), Toward the reconciliation of seismological and petrological perspectives on oceanic lithosphere heterogeneity, *Geochem. Geophys. Geosyst.*, *16*, 3129–3141, doi:10.1002/2015GC006017.

Received 15 JUL 2015
Accepted 2 SEP 2015
Accepted article online 7 SEP 2015
Published online 20 SEP 2015

1. Introduction

A distinctive feature of the seismic wavefield observed in the oceanic domain is the presence of high-frequency *Po* and *So* phases, whose onset travels with velocities characteristic of the mantle component of the lithosphere. These phases are recorded in many areas to very long distances from the source (3000 km or more) and are accompanied by complex coda [e.g., *Kennett and Furumura*, 2013]. Figure 1 illustrates the typical complex shape of *Po* and *So* arrivals for borehole OBS recordings from the Northwestern Pacific, with a record section constructed from a set of similar, shallow events along the Pacific plate margin from Izu-Bonin to the northern end of the Kurile arc. The traces are arranged in order of epicentral distance, aligned on the arrival of the *P* phase with amplitude normalized by the *S* arrival. All these events recorded at NWPAC1-3 (159.93°E, 41.12°N) display well-developed *Po* and *So* wave trains with high-frequency content and very long coda, but there are notable differences in the relative proportions of *Po* and *So* between events, and in the details of the shape of the envelope of the phases. For the closest event, *Po* has a rather distinct onset, but as the epicentral distance increases the *Po* envelopes for these paths show more of a spindle shape with the maximum amplitude occurring relatively late in the wave train. In all cases, *So* builds from a low start to a maximum and then has a long slow decay in the coda. At larger propagation distances, the *So* maximum tends to occur further into the wave train. Across the Northwest Pacific region, the apparent velocity for *Po* is 8.1 km/s and for *So* is 4.6 km/s. Similar properties as observed for regions of efficient *Po* and *So* propagation in other parts of the Pacific basin [*Kennett et al.*, 2014].

A significant role in generating complex seismic coda is played by the presence of the seawater and sediments [*Sereno and Orcutt*, 1985, 1987]. But, such a purely stratified structure produces rather distinct pulse-like arrivals rather than the continuous coda observed (as illustrated in *Kennett and Furumura* [2013, Figures 7c and 7d]). Further using just such 1-D variation requires a much stronger level of variability to produce the same strength of coda than is required for 2-D and 3-D heterogeneity [*Mallick and Frazer*, 1990; *Kennett and Furumura*, 2013].

Models which reproduce the character of the *Po* and *So* arrivals in 2-D simulations invoke quasi-laminar heterogeneity with a von-Kármán distribution characterized by horizontal correlation length 10–20 km and vertical correlation length 0.5 km in the mantle component of the lithosphere [*Kennett and Furumura*, 2013;

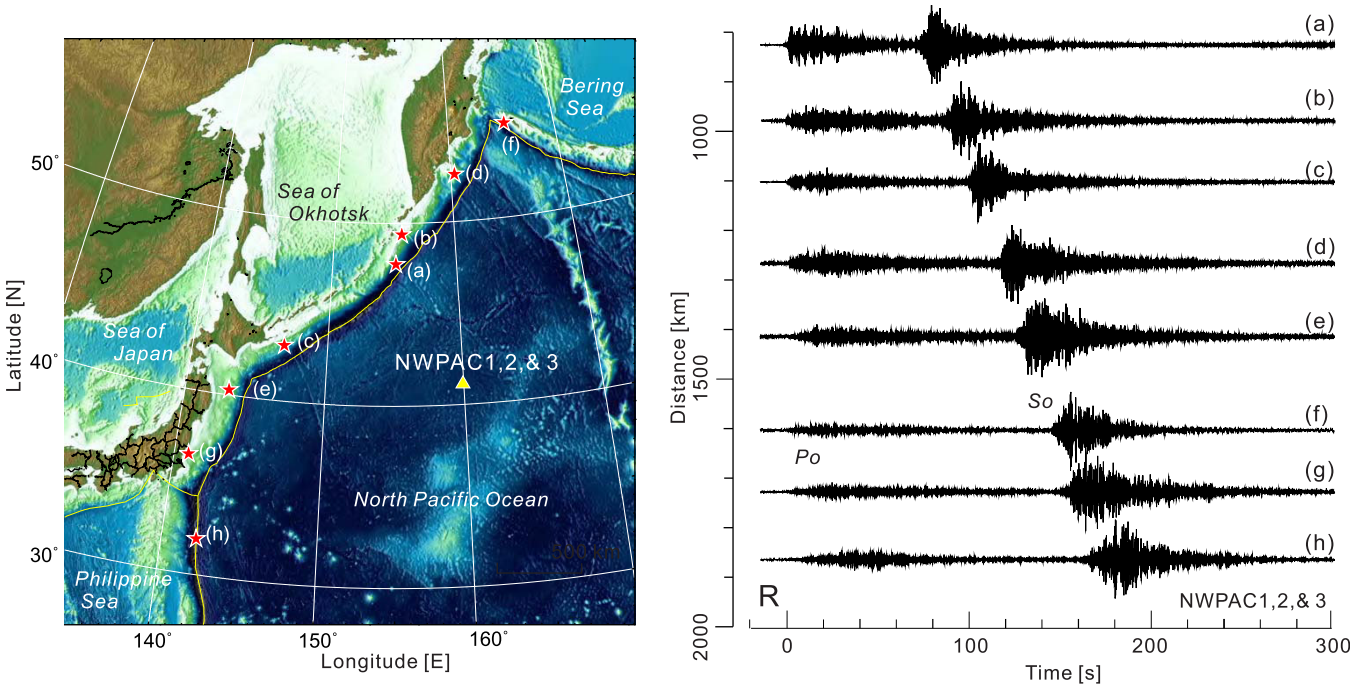

Figure 1. Record section of OBS records for *Po*, *So* phases recorded in the NW Pacific at stations NWPAC1, 2, and 3 (which operated in the same location, 159.93°E, 41.12°N, for different time periods); (left) map of events; (right) radial component records. The traces are ordered in increasing epicentral distance from the NWPAC station location.

Shito et al., 2013; *Chen et al*., 2013; *Kennett et al*., 2014]. The details of the crustal model have only a mild influence on the nature of the *Po* and *So* after propagation for a few hundred kilometers, because the seismic energy spends little time in this zone. To represent the sheeted dyke complex of oceanic crustal layer 3, *Kennett and Furumura* [2013] used a stochastic model with a longer vertical correlation length of 5 km with 0.25 km horizontally. This simple representation is common to all the cases presented in this paper.

The stochastic seismic models are designed to represent the character of seismograms after propagation through a substantial distance, and commonly assume a uniform level of heterogeneity through the lithosphere, or a concentration in the upper part that requires larger amounts of heterogeneity. The level of r.m.s. heterogeneity needed to match the character of the oceanic seismograms is typically 1–2% for uniform models [*Kennett and Furumura*, 2013; *Shito et al*., 2013].

Such quasi-laminar models were introduced by *Furumura and Kennett* [2005] to explain efficient guiding of high-frequency waves to the surface in subduction zone settings from events as deep as 500–600 km. *Shito et al*. [2013] have shown that they can model propagation from intermediate-depth earthquakes beneath Japan to broadband ocean-bottom-seismometers in the northwest Pacific using the same model for the oceanic lithosphere throughout, indicating that heterogeneity is acquired before subduction. It is possible that the heterogeneity may be modified during the process of bending the slab [*Garth and Rietbock*, 2014], but it needs to be present in the oceanic lithosphere before subduction.

The broad-scale distributed heterogeneity introduced in the seismic models is difficult to explain with standard petrological models. Hence, *Shito et al*. [2013] suggest lamination of pyroxenite and/or chromitite layers in oceanic peridotite, though such veins in exposed mantle sections of ophiolites are on a much smaller scale.

The observation of *Kennett et al*. [2014] of less efficient *Po* and *So* propagation in younger lithosphere (higher temperatures and attenuation) would be consistent with the introduction of heterogeneity in the general neighborhood of the ridge crest, with contrasts masked by the presence of strong attenuation but having a stronger influence on the wavefield as the lithosphere cools.

Kawakatsu et al. [2009] have proposed the presence of a "mille-feuile" structure in the oceanic asthenosphere, with elongated pods of partial melt, to explain the contrasts with the lithosphere seen in *S* wave

receiver function studies at ocean bottom seismometers. The quasi-laminate heterogeneity structures proposed for the oceanic lithosphere have a strong resemblance to these asthenospheric structures, but with reduced contrast as would be produced by freezing the melt.

From the detailed study by *Hirschmann* [2010] of the nature of the melt distribution in the asthenosphere beneath the oceans, such *frozen* material would be largely expected to underplate the oceanic lithosphere, rather than to be incorporated into it. Both former melt and heterogeneity due to the presence of elongate enriched domains are likely to be concentrated toward the base of the lithosphere. Such a distribution is at odds with present seismic heterogeneity models, but can the different concepts of structure be reconciled?

2. Petrological Heterogeneity

Most work on petrological and geochemical heterogeneity is based on analyses of physical samples. In the oceanic domains this means that sampling is concentrated at or near the mid-ocean ridges, supplemented by limited information from peridotitic xenoliths away from the ridge. Usually, the xenoliths are associated with oceanic islands, which themselves represent tangible evidence for heterogeneity.

Along the mid-ocean ridges the geochemical signatures of erupted mid-ocean-ridge basalts (MORB) provide evidence for heterogeneous sources on relatively short spatial scales [e.g., *Rubin et al*., 2009]. The properties of MORB appear to be more homogenized for faster spreading ridges. Such crustal products represent the effusion from the mid-ocean-ridge volcanoes and so carry an indistinct imprint of the particular processes and plumbing regime that is building the mantle component beneath. It is likely that sills are emplaced below crustal levels near the axis of spreading, though there appears to be little constraint on their likely size. In the dominantly peridotitic mixture that upwells below the ridge site, there will be other components such as pyroxenite that have the potential to be included into the lithospheric mantle. Further away from the ridge such enriched domains can be expected to be stretched into elongate domains with high aspect ratio as a consequence of the divergence in flow away from the ridge area [*Allégre and Turcotte*, 1986].

Models for the evolution of the oceanic lithosphere are based on the cooling of homogeneous material, even when sophisticated representations of material properties are used [e.g., *Grose and Afonso*, 2013]. Any fine-scale heterogeneity will simply be absorbed into a mixed assemblage, whose overall properties are used to assess major trends. The impact of the levels of fluctuation in physical properties proposed in the seismic models will be much less than the differences between different styles of cooling models.

The most direct representation of the likely character of the oceanic over the broad spectrum of lithospheric ages comes from the analysis of melting scenarios [*Hirschmann*, 2010], taking into account the way in which minor components of the mantle upwelling can have a profound effect on melting. The major zone where partial melt will be present comes from depressurization melting below the vicinity of the ridge crest in a zone that approximately scales with spreading rate. Infusion of minor melt components into the lithospheric mantle is thus more likely to occur some distance away from the ridge on a fast spreading ridge, such as the current East Pacific Rise. Seismic reflection experiments have detected off-axis features interpreted as containing melt in the oceanic crust [e.g., *Han et al*., 2014], but would not have the capacity to illuminate any equivalent features in the mantle beneath.

Melting away from the ridge would be expected to have a minor effect with any local melt lenses freezing eventually onto the base of the lithosphere. The models of *Hirschmann* [2010] indicate that the melt regime below the growing oceanic plate, with a steady state influx of hotter material near the ridge coming from depth, will vary with lithospheric age, as a function of the pressure and temperature at base of the cooling plate. Silicate melts will dominate below the lithosphere out to $\sim$30 Ma, by which time the plate will be about 50 km thick. For greater ages, carbonatite melts will be stable below the oceanic lithosphere. Melting just below older lithosphere would be expected to be associated with compaction melt from the underlying asthenosphere, but might be enhanced by replenishment from plumes or small-scale convection. Larger volumes of melt infusion might arise from enriched heterogeneities, such as pyroxenites [*Hirschmann*, 2010]. Thus away from the ridge area the addition of melt is expected to be at the base of the growing lithosphere, with the possibility of building up a moderate thickness of heterogeneous material for old

plates such as are found in the northwest and southwest Pacific where the seismic phases *Po* and *So* are very clearly observed.

The scales of petrological heterogeneity are difficult to address, since most physical specimens related to the mantle are small. Nevertheless, there are strong indications of mineralogical heterogeneity from the microscale to the largest features found in outcrop. *Tommasi and Ishikawa* [2014] have presented a detailed analysis of xenolith samples from the Solomon Islands sampling material from the Ontong Jave plateau. The material down to 85 km is thought to be related to the former Pacific plate rather than the subsequent modification by plume influence. This upper zone shows variations in Vp and Vs from the lherzolitic components of around 2% on a small scale with much higher seismic wave speeds associated with the pyroxenites. The textural analysis by *Tommasi and Ishikawa* [2014] suggest that the aggregate properties will show little anisotropy, and so noticeable velocity variations are most likely due to localized chemical differentiation.

However, even exhumed peridotite massifs or basal (mantle) parts of ophiolites that show lamination do so at the meter scale. In most cases, the exposures are not large enough for kilometer-scale features to become evident, particularly since the broader-scale variations most likely arise from the cumulative effect of many smaller features. Subtle and gradual changes in physical properties may also not have a distinctive character in the field.

3. Seismological Heterogeneity

The seismological models derived from the high-frequency observations of *Po* and *So* after propagation through considerable distances represent aggregate models for these long paths, and are hence confined to description of the general behavior rather than any specific localization. The limited range of receiver functions carried out using OBS average out any detail in the lithosphere by employing moderate frequencies (around 0.1 Hz) to avoid noise issues [*Kawakatsu et al*., 2009] and so have low vertical resolution. The receiver function methods are sensitive to significant contrasts in physical properties and have not registered any internal lithospheric discontinuities beside the Moho.

With dense observations, it can be feasible to construct deterministic models of complex seismic structure to even a fine scale, but such dense sampling is not currently available in the oceanic domain. The complex nature of high-frequency observations on many different paths means that the results are only amenable to description by stochastic models. In such models the wave number spectrum of heterogeneity is controlled by a few parameters. A convenient form that allows significant short-scale heterogeneity is provided by the von Kármán distribution [see e.g., *Ishimaru*, 1987]. In 2-D, this probability density distribution for fluctuations in seismic wave speed is specified in terms of horizontal slowness p and vertical slowness q as

$$P(p,q)=\frac{4\pi\kappa\epsilon^2 a_x a_z}{\left(1+\omega^2 a_x^2 p^2+\omega^2 a_z^2 q^2\right)^{\kappa+1}}\,, \tag{1}$$

using differing correlation lengths a_x in the horizontal and a_z in the vertical direction, and an r.m.s. amplitude of wave speed deviation from the reference ϵ. κ is the Hurst exponent that specifies the rate of decrease of short wavelength features and a typical value is 0.5. This power spectrum describes a full ensemble of models, but as soon as we need to implement a model for numerical implementation we work with just a single realization. Fortunately, the main characteristics of the seismic wavefield are stable with respect to specific realizations, but each realization brings its own specific properties.

In this study we use κ=0.5, which introduces a fair amount of short-scale heterogeneity. Various values of κ ranging from 0.3 to 0.8 have been estimated for the continental lithosphere, particularly the crust [see e.g., *Sato et al*., 2012], but there are no comparable studies for the oceanic lithosphere. *Shearer and Earle* [2004] find that κ=0.5 provides a good general description of the properties of the lithosphere from studies of teleseismic scattering across the globe.

The high-frequency *Po* and *So* wavefield in the observations has a strong 3-D component with, e.g., almost equal strength of the radial and transverse component for *P* waves after just a few seconds from the onset of the wave train. However, simulations that can encompass a wide variety of models for long-distance

propagation are restricted to just 2-D models because of the computational expense for high frequencies. The comparisons made by *Kennett and Furumura* [2008] between 2-D and 3-D simulations for modest size models (about 250 km across) suggest that the 2-D results can provide a reasonable representation of the character of the wavefield. The slower geometrical spreading in 2-D tends to compensate for the out-of-plane effects in 3-D, but there is a tendency for an apparently longer coda in the 2-D simulation since the later arrivals at larger propagation distances do not attenuate so quickly as in 3-D.

Even so, direct comparison of 2-D simulations with observed seismograms is difficult, since we do not know whether the actual "grain" of the structures in 3-D lends itself to a 2-D representation, and the extended coda may be misleading. *Kennett and Furumura* [2013] have investigated the way in which the wavefield is built up through the inclusion of increasing levels of complexity, and have shown how to capture the general character of the *Po* and *So* observations.

Shito et al. [2013] use matching of envelopes between 2-D simulations and a set of seismic observations for intermediate-depth earthquakes beneath Japan recorded at a cluster of ocean bottom seismometers in the northwest Pacific. From the envelope matches they extract a set of stochastic parameters by a grid search. Even though the envelope of the wave trains is a relatively stable feature, there are variations between realizations of the heterogeneous media, and trade-offs with external factors such as the assumed level of intrinsic seismic attenuation. Indeed the relative stability of the envelope to changes in the stochastic parameters means that optimization is difficult since the areas of good fit in parameter space are broad. The estimated values obtained by *Shito et al*. [2013] for the correlation lengths, 10 km horizontally and 0.5 km vertically with an amplitude of heterogeneity of 2%, are consistent with those inferred by *Kennett and Furumura* [2013] by matching the general character of waveforms on a larger collection of paths.

Kennett and Furumura [2013] have shown how models with a uniform distribution of stochastic heterogeneity through the mantle component of the oceanic lithosphere can provide a good representation of the general character of the high-frequency phases *Po* and *So* as seen on many different paths in the relatively old lithosphere of the north-western Pacific. Purely stratified models produce rather distinctive multiple minor pulses that can be broken up into a more continuous coda by replacement with stochastic heterogeneity. The introduction of much longer horizontal correlation length than in the vertical direction has the effect of sustaining the coda both in duration and in persistence to larger distances through enhancement of multiple scattered and diffraction processes that preferentially direct energy in the forward direction. The uniform distribution of heterogeneity with depth through the mantle lithosphere was chosen on the grounds of simplicity and provides a good representation of *Po* and *So* behavior without invoking large physical contrasts (r.m.s. amplitude of stochastic variation 2%). The work of *Shito et al*. [2013] demonstrates that the same model of heterogeneity is applicable in the old oceanic lithosphere of the NW Pacific and in the subducting Pacific plate beneath Japan

A similar uniform distribution of heterogeneity (amplitude 2%) has been used by *Shito et al*. [2015] in a study of *Po* and *So* propagation in the much younger lithosphere of the Philippine Sea plate. They note systematic thickening of the lithosphere with increasing age, and favor an even longer horizontal correlation length than for the northwest Pacific. For this young lithosphere ($<$45 Ma), the effects of intrinsic attenuation are also important, and there are trade-offs between the intrinsic attenuation model and the heterogeneity structure that induces scattering attenuation.

In Figure 2a, we show the results of a 2-D numerical simulation with a uniform level of stochastic heterogeneity of 2% through the mantle component of a 100 km thick oceanic lithosphere (correlation length: 10 km horizontally and 0.5 km vertically), using the same approach as in *Kennett and Furumura* [2013]. The top figure shows record sections for both radial and vertical components, and below we show representative snapshots of the wavefield. The base model has weak gradients for both *P* and *S* wave speeds so that the dominant mode of ducting energy to large distances is via multiple scattering in the heterogeneous medium. Once established the multiple scattering wavefield is very robust. This means that a broad range of heterogeneous structure will produce similar wavefields. As demonstrated by *Kennett et al*. [2014], even major changes in lithospheric thickness have only a modest impact on the transmission of *Po* and *So* energy. Nevertheless, the scattered field is quite sensitive to intrinsic attenuation and is rapidly diminished where temperatures are higher and attenuation is increased.

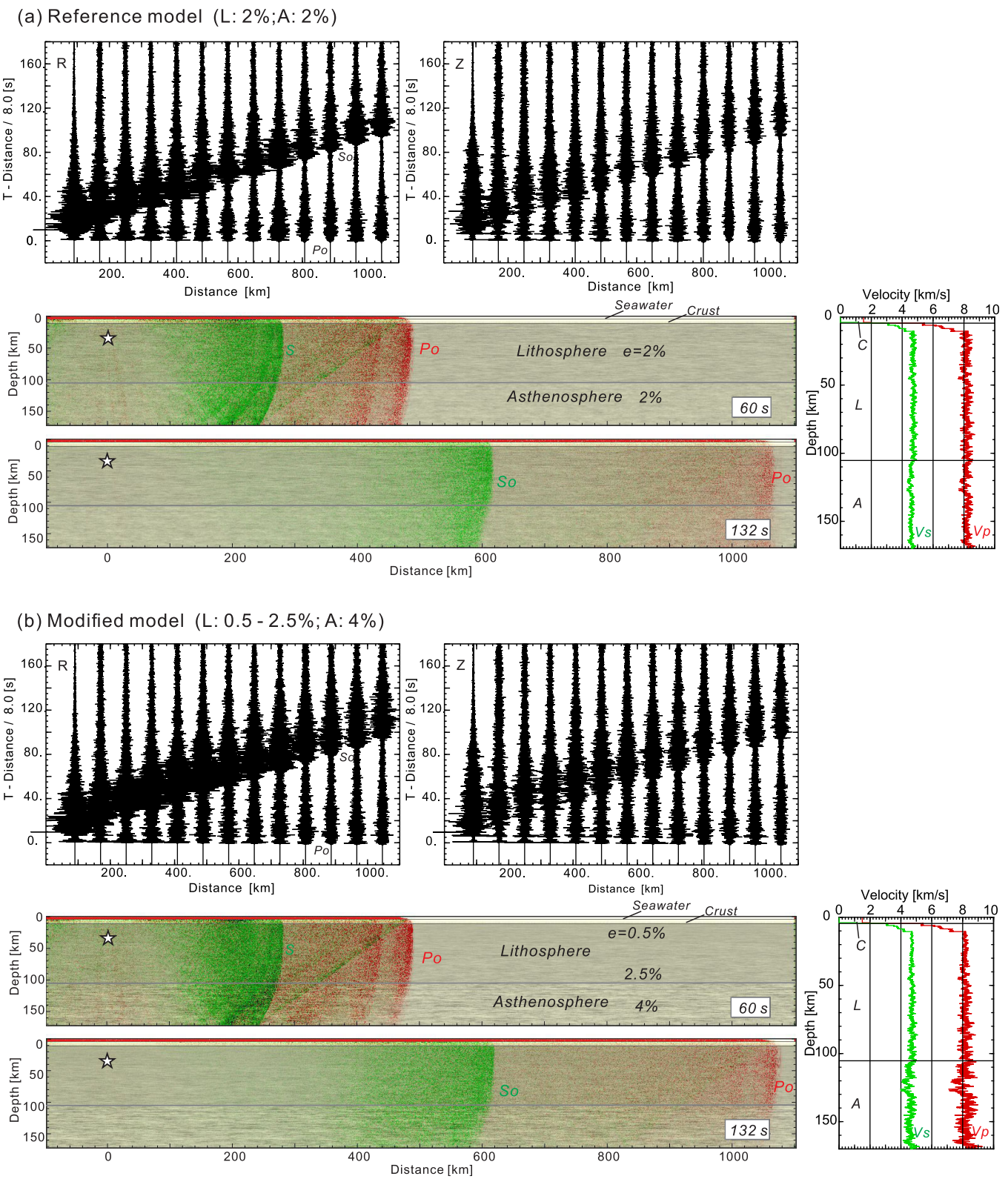

Figure 2. Record sections and snapshots for *Po* and *So* wave propagation. (a) Reference case with uniform stochastic heterogeneity in the lithosphere and asthenosphere at a level of 2%. (b) Modified model with a sinusoidal variation of heterogeneity amplitude from 0.5% at the top of the mantle to 2.5% at the base of the lithosphere, with 4% heterogeneity in the asthenosphere. In each case, we have used a horizontal correlation length of 10 km and vertical correlation length of 0.5 km with a von Kármán distribution of heterogeneity. One-dimensional profiles at the midpoint location are shown to the right of the snapshots.

In light of the petrological information that suggests that heterogeneity is likely to be added preferentially to the ageing lithosphere from below, we have investigated how far the vertical distribution of heterogeneity can be modified and still achieve a suitable representation of the character of the high-frequency wave propagation. In Figure 2b, we show a simple modification of the heterogeneity regime in which we have imposed a sinusoidal variation in heterogeneity amplitude from 0.5% at the top of the mantle to 2.5% at the base of the lithosphere, with 4% heterogeneity in the asthenosphere beneath. The change in the wavefield from the reference case in Figure 2a is small over the full distance span. A subtle feature visible in the snapshots is that the onset of the *Po* and *So* wavefronts become more broken at the base of the lithosphere when heterogeneity is concentrated there. Scattering in enhanced heterogeneity reinforces the scattered field, but the main ducting of energy occurs in the zones with slightly less heterogeneity. If the heterogeneity in the asthenosphere is reduced to 2% (as in the reference case), the rate of decay of the coda of the *Po* and *So* phases is slightly faster, but there is little change to the general appearance (Figure 3a). In contrast, when we place stronger heterogeneity in the shallow part of the lithosphere with weaker heterogeneity beneath, the rate of decay of the amplitudes of the high-frequency phases with distance is faster than in the reference case, particularly for *So*, as illustrated in Figure 3b.

It is necessary to keep a modest level of heterogeneity (around 0.5%) at the top of the mantle lithosphere, or else the simulated wavefield becomes too "spiky," with very distinct pulses rather than the continuous coda that is seen in the observations (cf. Figure 1).

We show in Figure 4 the variation in the envelope of the *Po* and *So* phases for the models in Figures 2 and 3, at propagation distances of 500 and 1000 km. The influence of the different styles of heterogeneity is most marked on the vertical (Z) component, on which we can clearly see the relative suppression of *So* in the circumstance with heterogeneity concentrated in the upper part of the lithospheric mantle (d). The envelopes for the bottom-weighted cases (b, c) are more similar to the base model (a) with uniformly distributed heterogeneity, but have sharper onsets for *Po*. Enhanced heterogeneity in the asthenosphere tends to return additional high-frequency energy to the lithosphere, unless there is strong intrinsic attenuation in this zone.

We have also undertaken numerical simulations for guided wave propagation from deep sources in subduction zones (Figure 5), and once again there is little difference in the behavior for a uniform distribution of heterogeneity as considered by *Furumura and Kennett* [2005] and a bottom-weighted distribution similar to the example in Figure 2b. The observations at the surface are again for long distance travel in the complex medium and provide little discrimination for the detailed distribution of the heterogeneity distribution, though favoring scenarios with elongate correlation length along the slab.

For the 2-D simulation on a section through the subducting Pacific plate beneath Hokkaido, the uniform model (Figure 5b) and the bottom-weighted model (Figure 5c) give stronger high-frequency guiding and more complex coda that heterogeneity concentrated near the top of the plate (Figure 5d). *Sun et al.* [2014] in a study of high-frequency guided waves in the Calabrian slab beneath southern Italy have again found that uniform quasi-laminate heterogeneity with elongate correlation length along the slab provides a good representation of observations for stations lying above the steeply dipping (79°) portion of the slab. The shallower part of the slab only dips at 20°, and the stations are likely to sample energy emerging from the upper part of the slab. Suppression of heterogeneity in the bottom half of the Calabrian slab still leaves significant guided energy at the surface stations, but the coda is dramatically reduced if the heterogeneity in the upper part of the slab is removed. We have noted above the need to retain some level of heterogeneity throughout the oceanic lithosphere to sustain appropriate character in the *Po* and *So* arrivals. Reintroduction of modest heterogeneity into the upper part of the slab for the *Sun et al.* [2014] models would be expected to reinvigorate the high-frequency *Po* coda even when heterogeneity is concentrated in the bottom part.

4. Discussion and Conclusions

With due recognition of the assumptions and limitations of stochastic models, we have been able to produce a style of seismic model that is in closer correspondence with petrological expectations. Although the heterogeneous seismic model is isotropic, when viewed with longer period waves, e.g. surface waves, the structures will appear to show radial anisotropy.

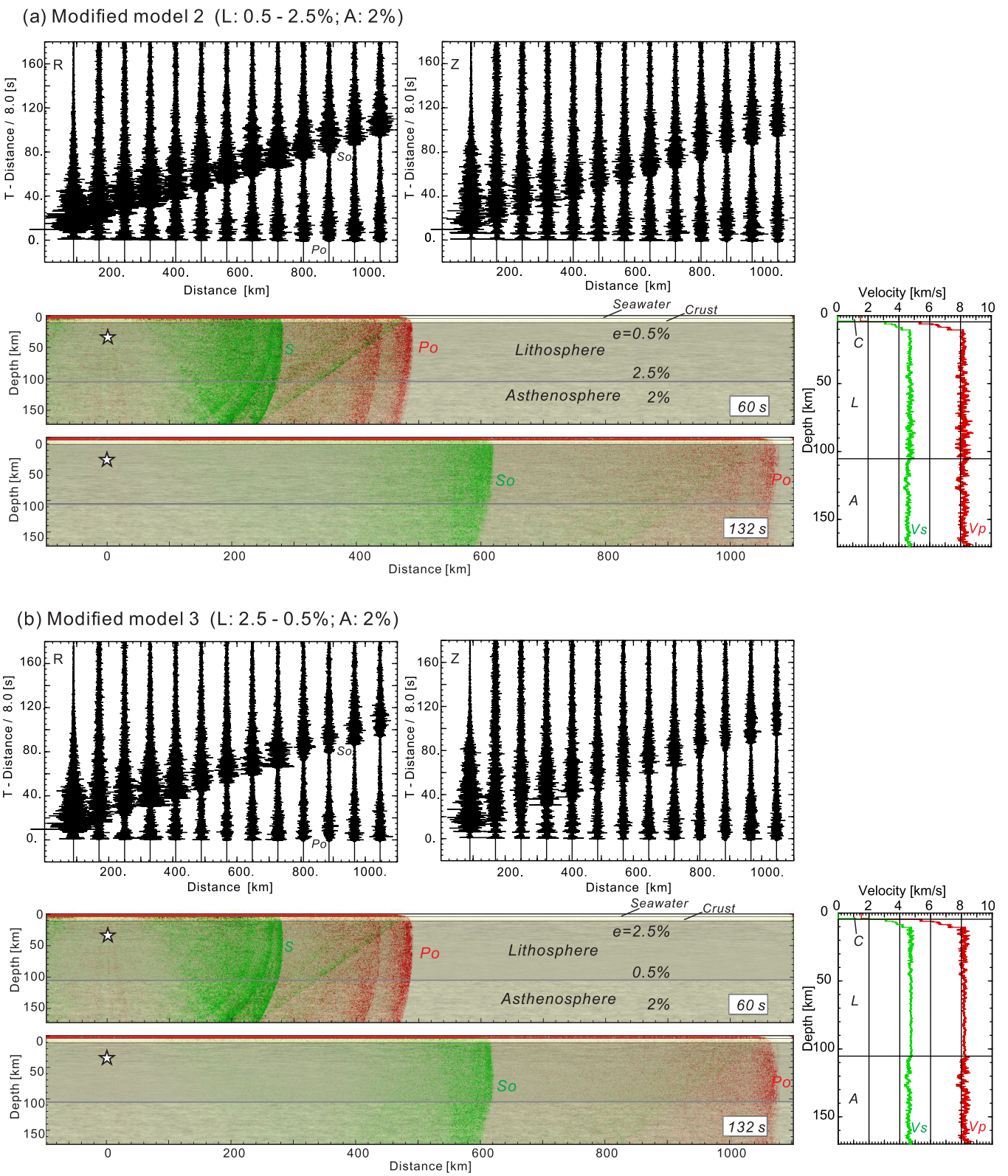

Figure 3. Comparison of record sections and snapshots for *Po* and *So* wave propagation with varying heterogeneity in the lithosphere and heterogeneity amplitude of 2% in the asthenosphere, with the same class of quasi-laminate heterogeneity as in Figure 2. (a) Bottom-weighted heterogeneity with a sinusoidal variation of heterogeneity from 0.5% at the top of the mantle to 2.5% at the base of the lithosphere. (b) Top-weighted heterogeneity with a sinusoidal variation of heterogeneity from 2.5% at the top of the mantle to 0.5% at the base of the lithosphere. One-dimensional profiles at the midpoint location are shown to the right of the snapshots.

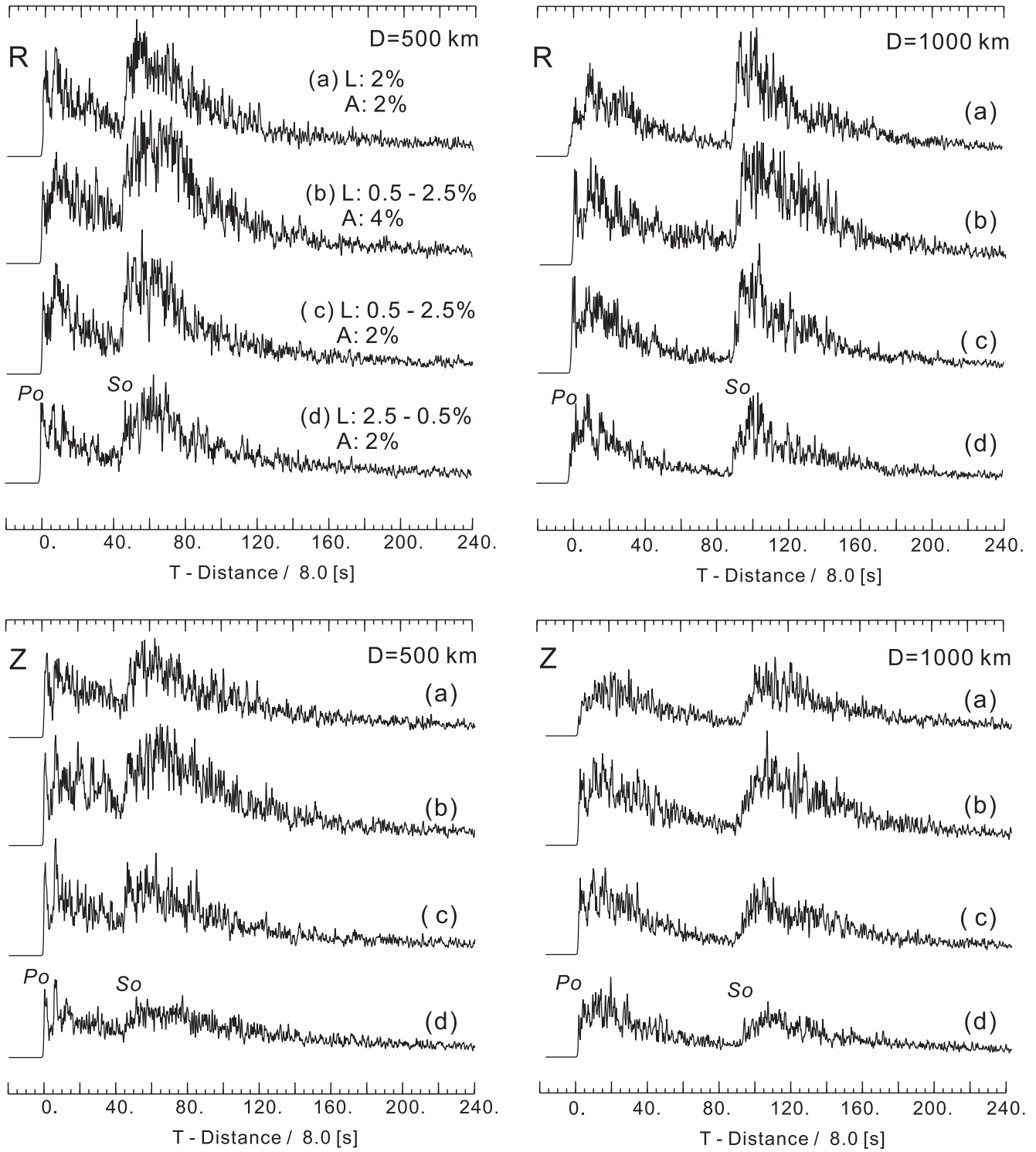

Figure 4. Envelopes for the radial (R) and vertical (Z) components of *Po* and *So* for the models considered in Figures 2 and 3. (a) Uniform 2% stochastic heterogeneity in the lithosphere and asthenosphere; (b) 4% heterogeneity in the asthenosphere and a sinusoidal variation of heterogeneity from 0.5% at the top of the mantle to 2.5% at the base of the lithosphere; (c) 2% heterogeneity in the asthenosphere and a sinusoidal variation of heterogeneity from 0.5% at the top of the mantle to 2.5% at the base of the lithosphere; (d) 2% heterogeneity in the asthenosphere and a sinusoidal variation of heterogeneity from 2.5% at the top of the mantle to 0.5% at the base of the lithosphere.

A finely laminated set of isotropic materials in a 1-D model appears to be transversely isotropic when traversed by seismic wavelengths which are long compared to the thickness of the individual layers [see e.g., *Backus*, 1962; *Fichtner et al.*, 2013]. In a similar way, a random medium with laterally elongated

heterogeneities is macroscopically equivalent to a transversely isotropic medium with slightly faster wave speed parallel to the quasi-laminate structure [e.g., *Saito*, 2006]. Numerical simulations for various quasi-laminate structures illustrating the directional dependence are shown by *Furumura and Kennett* [2008, Figures 6 and 7]. The apparent level of radial anisotropy increases with the level of variation in the quasi-laminate heterogeneity and is typically of the order of about a half of the r.m.s. amplitude for correlation length ratios greater than 10. For sampling by very long waves, many local realizations of the heterogeneity will be traversed in a wavelength and the net effect will be equivalent to an ensemble average.

The laterally varying quasi-laminate heterogeneity with elongate horizontal correlation, as displayed in Figures 2–4, will average to a structure with somewhat faster horizontally polarized shear wave speed V_{SH} than vertically polarized $V_{SV.}$ In the model presented in Figure 2b the strength of the radial anisotropy $\xi=[V_{SH}/V_{SV}]^2$, associated with the heterogeneity, will increase with depth through the mantle component of the lithosphere with a maximum gradient at a depth around 60 km, for 100 km thick lithosphere.

Burgos et al. [2014] have made a comprehensive survey of the ocean basins using surface wave dispersion for Rayleigh and Love waves. They employ a number of different proxies for the possible location of the lithosphere/asthenosphere boundary (LAB) based on seismic wave speed, radial anisotropy, and azimuthal anisotropy. *Burgos et al*. [2014] note that for most of the oceans the criterion based on the maximum gradient of the parameter ξ occurs at a near constant depth near 60 km, somewhat shallower than the estimate from the peak negative gradient of $V_{SV.}$ The presence of a sharp change in radial anisotropy is suggestive of processes associated with underplating of the lithosphere. The values of ξ determined by *Burgos et al*. [2014] are rather larger than could be produced by the class of heterogeneity compatible with the *Po* and *So* observations, but the heterogeneity could help to enhance intrinsic anisotropic effects. The near constant depth for the maximum ξ gradient might reflect a change in the physical properties of the lithospheric material, associated with a change in the freezing regime for underplating melts as a function of lithospheric age.

Sun et al. [2014] have assessed the range of processes that could produce distributed quasi-laminar heterogeneity in the oceanic lithosphere. They favor an origin in processes near the mid-ocean ridge that could produce melt-rich bands that ultimately freeze, and interaction with the thickening oceanic lithosphere as it moves away from the ridge, including melt confined to a gently dipping decompaction channel at the base. The relative shear flow with the asthenosphere will tend to produce near horizontal alignment which can then be preserved as the material continues to be transported further away from the ridge. The most likely scale lengths are those associated with the dimensions of ridge magma chambers, and thus around 10 km or more, which is consistent with the inferred correlation lengths.

The initially modest level of heterogeneity can then be supplemented by the underplating processes well away from the mid-ocean ridge, and thereby produce a more complex, bottom-weighted heterogeneity profile in the mature lithosphere. In the melting models of *Hirschmann* [2010] out to about 30 Ma with a lithosphere thickness around 50–60 km, silicate melts would be stable beneath the lithosphere and thereafter would be replaced by carbonatite melt. The shallower part of the lithosphere which is emplaced by 30 Ma with weak intrinsic variability as a function of near ridge crest processes would acquire a gradation in properties as successive underplating occurs, with occasional incorporation of chemically distinct materials such as pyroxenite. Once the melt regime changes, a different style of underplating will come into play that could leave a distinct trace in the gradient of anisotropy.

Enriched heterogeneities are likely to become even more stretched further way from the ridge, since they will have spent longer in a divergent flow field, before being attached to older lithosphere. The inclusion of chemically distinct heterogeneity via freezing material onto the base of the lithosphere also provides a way of enhancing wave speed contrasts, because of the much larger water uptake by pyroxene than olivine under lithospheric conditions [*Dai and Karato*, 2009]. Changes in water content are also likely to influence the rheology through activation of different deformation mechanisms without reaching melting conditions [*Olugboji et al*., 2013].

In a study exploiting the properties of precursors to the phase *SS* which highlight discontinuities below the region of the surface bounce point, *Schmerr* [2012] has employed acceleration waveforms to improve resolution. He has identified considerable variations in the nature of the transition from lithosphere to asthenosphere, with an identification of the sharpest changes as associated with melts. Variations in the sharpness

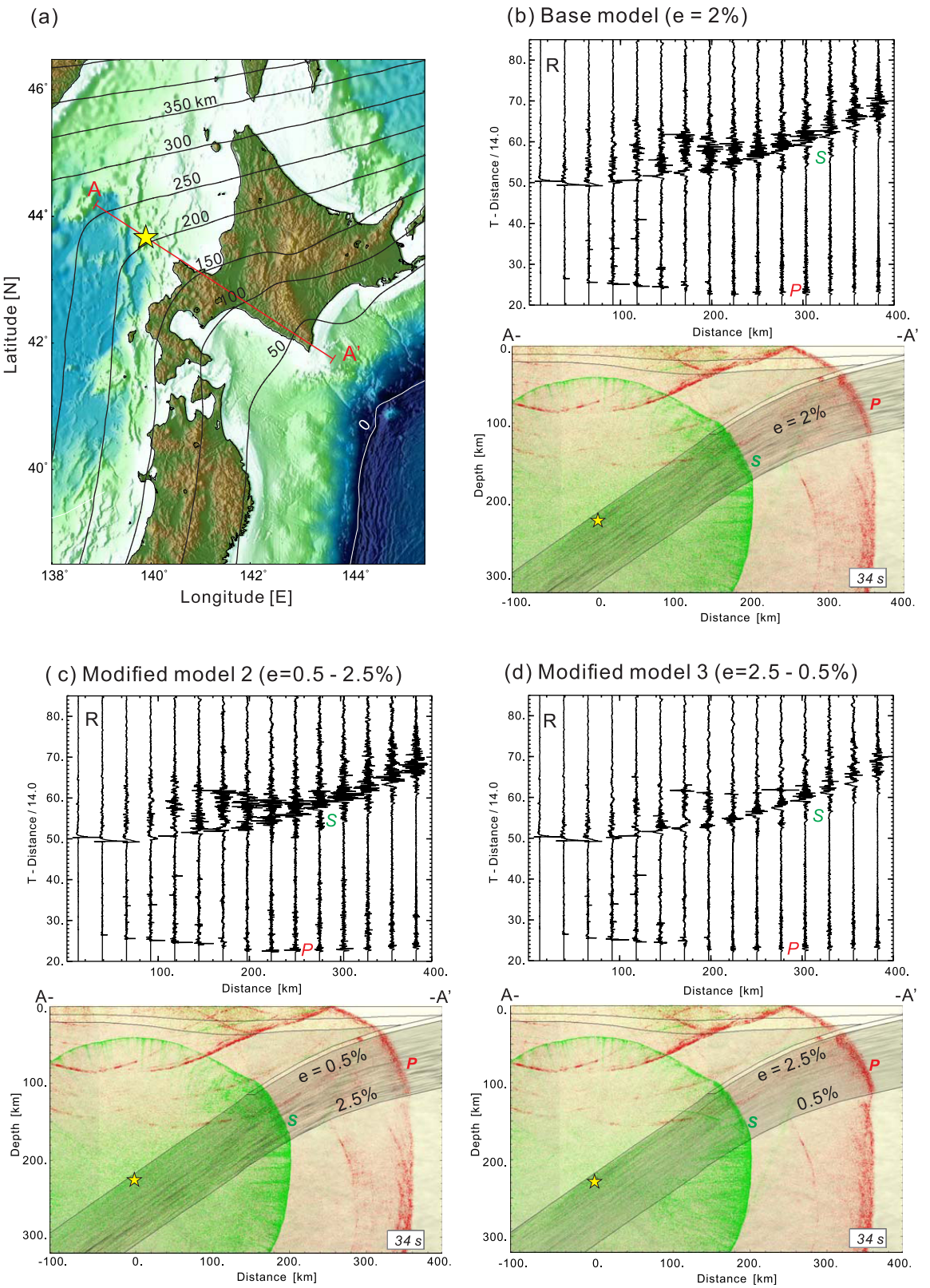

Figure 5. (a) Two-dimensional modeling of *P* and *S* guided waves in subducted lithosphere with a profile taken along A-A′ across Hokkaido, Japan. Record sections of radial component seismograms and snapshots, at 34 s after source initiation, are shown for three models. (b) Base model with 2% heterogeneity through the full thickness of the subducted plate. (c) Modified model with sinusoidal heterogeneous amplitude from 0.5% at the top of the slab to 2.5% at the base. (d) Inverse model with sinusoidal heterogeneous amplitude from 2.5% at the top of the slab to 0.5% at the base.

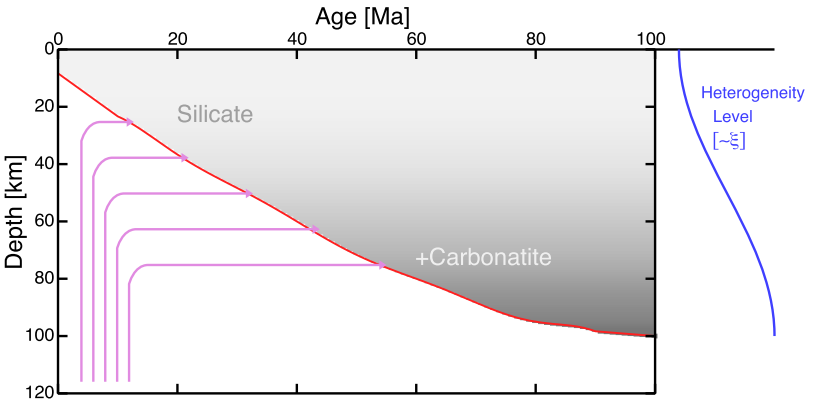

Figure 6. Schematic view of possible heterogeneity in the oceanic lithosphere associated with growth by cooling and influx of new material through the neighborhood of the ridge crest. The heterogeneity level represents the likely amplitude of fluctuations in oceanic wave speed with a quasi-laminate configuration, which would be linked to radial anisotropy ξ.

of the lithosphere boundary will affect the retention of multiple scattered energy. Much more will escape with a gradual transition, thereby decreasing the efficiency of propagation of *Po* and *So*. Such influences appear to tie to some localized variations in the propagation characteristics across the Pacific Basin [*Kennett et al*., 2014] that appear to contradict major trends. An example is the zone near Midway Island where no lithosphere boundary can be recognized in the study by *Schmerr* [2012], paths crossing through this region of moderately old lithosphere show much less clear *So* than in other parts of the northern Pacific [*Kennett et al*., 2014, Figure 1].

In simulations of receiver functions, models with variable quasi-laminate heterogeneity can produce apparent discontinuities at abrupt changes in either heterogeneity amplitude or correlation properties, but these are always of modest size and by themselves insufficient to explain the class of velocity drop seen in, e.g., the work of *Kawakatsu et al*. [2009] without augmentation of the velocity contrast by melt. However, such changes may be linked to mild internal discontinuities in the lithosphere such as the rapid change in radial anisotropy noted by *Burgos et al*. [2014] at a similar depth to the most rapid change in heterogeneity properties in Figure 2b.

The original stochastic models for heterogeneity in the lithosphere used a uniform vertical distribution since this was compatible with the observations of the high-frequency phases. We have shown that it possible to produce a modified model for older lithosphere that retains a suitable representation of the observed seismograms, but now places greater heterogeneity at the base of the lithosphere where it might be introduced by underplating. The modified profile also links to the noticeable gradients in radial anisotropy in the oceanic lithosphere inferred from analysis of surface wave dispersion, though was not designed for this purpose. The main difference from petrological concepts rests with the scale lengths of the inferred seismic heterogeneity compared with available exposures of mantle material. It remains to be seen whether further evidence can be found for kilometer-scale variations in physical properties, which would close the gap between the different disciplinary perspectives even further.

Figure 6 presents a schematic rendering of a plausible scenario for oceanic lithosphere heterogeneity combining both seismological and petrological information. Ascending flow near the ridge will divert sideways to impinge on the growing lithosphere bringing melts and heterogeneities that are then incorporated into the lithospheric mantle. For younger lithosphere underplating will be via silicate melts but beyond 30 Ma carbonatite melts can be frozen in *Hirschmann* [2010]. The change in regime may well lead to a higher level of quasi-laminate heterogeneity at depth. The heterogeneity level can be viewed as a potential proxy for radial anisotropy (ξ), so that the change in gradient reflects the inflexion noted from surface wave studies.

Acknowledgments
This work was stimulated by discussions at the Normal Mantle Workshop held in Matsushima, Japan in March 2015, organized by H. Utada and H. Kawakatsu. In the various discussions it became clear that the gulf between different viewpoints on the nature of heterogeneity might be bridgeable, and this paper is an attempt to build on that concept. We thank the Ocean Hemisphere Project Data Management Center (OHPDMC) at the Earthquake Research Institute, the University of Tokyo for providing the data from borehole broadband ocean bottom seismometer illustrated in Figure 1.

References

Allégre, C. J., and D. L. Turcotte (1986), Implications of a two component marble-cake mantle, *Nature*, *323*, 123–127.
Backus, G. E. (1962), Long-wave elastic anisotropy produced by horizontal layering, *J. Geophys. Res.*, *67*, 4427–4440.
Burgos, G., J.-P. Montagner, E. Beucler, Y. Capdeville, A. Mocquet, and M. Drilleau (2014), Oceanic lithosphere/asthenosphere boundary from surface wave dispersion data, *J. Geophys. Res. Solid Earth*, *119*, 1079–1093, doi:10.1002/2013JB010528.

Chen, K. H., B. L. N. Kennett, and T. Furumura (2013), High frequency waves guided by the subducted plates underneath Taiwan and their association with seismic intensity anomalies, *J. Geophys. Res. Solid Earth*, *118*, 665–680, doi:10.1002/jgrb.50071.

Dai, L., and S.-I. Karato (2009), Electrical conductivity of orthopyroxene: Implications for the water content of the asthenosphere, *Proc. Jpn. Acad., Ser. B*, *85*, 466–475.

Fichtner, A., B. L. N. Kennett, and J. Trampert (2013), Separating intrinsic and apparent anisotropy, *Phys. Earth Planet. Inter.*, *219*, 11–20, doi:10.1016/j.pepi.2013.03.006.

Furumura, T., and B. L. N. Kennett (2005), Subduction zone guided waves and the heterogeneity structure of the subducted plate: Intensity anomalies in northern Japan, *J. Geophys. Res.*, *110*, B10302, doi:10.1029/2004JB003486.

Furumura, T., and B. L. N. Kennett (2008), A scattering waveguide in the heterogeneous subducting plate, in *Scattering of Short-Period Seismic Waves in Earth Heterogeneity, Adv. Geophys.*, vol. 50, edited by H. Sato and M. Fehler, pp. 195–217, Academic, N. Y.

Garth, T., and A. Rietbock (2014), Order of magnitude increase in subducted H_2O due to hydrated normal faults with the Wadachi-Benioff zone, *Geology*, *42*, 207–210, doi:10.1130/G34730.1.

Grose, C. J., and J. C. Afonso (2013), Comprehensive plate models for the thermal evolution of oceanic lithosphere, *Geochem. Geophys. Geosyst.*, *14*, 3751–3778, doi:10.1002/ggge.20232.

Han, S., S. M. Carbotte, H. Carton, J. C. Mutter, O. Aghaei, M. R. Nedimović, and J. P. Canales (2014), Architecture of on- and off-axis magma bodies at EPR 9°37-40′N and implications for oceanic crustal accretion, *Earth Planet. Sci. Lett.*, *390*, 31–44, doi:10.1016/j.epsl.2013.12.040.

Hirschmann, M. M. (2010), Partial melt in the oceanic low velocity zone, *Phys. Earth Planet. Inter.*, *179*, 60–71.

Ishimaru, A. (1987), *Wave Propagation and Scattering in Random Media*, Academic, N. Y.

Kawakatsu, H., P. Kumar, Y. Takei, M. Shinohara, T. Kanazawa, E. Araki, and K. Suyehiro (2009), Seismic evidence for sharp lithosphere-asthenosphere boundaries of oceanic plates, *Science*, *324*, 499–502.

Kennett, B. L. N., and T. Furumura (2008), Stochastic waveguide in the Lithosphere: Indonesian subduction zone to Australian Craton, *Geophys. J. Int.*, *172*, 363–382.

Kennett, B. L. N., and T. Furumura (2013), High-frequency *Po*/*So* guided waves in the oceanic lithosphere: I—Long distance propagation, *Geophys. J. Int.*, *195*, 1862–1877.

Kennett, B. L. N., T. Furumura, and Y. Zhao (2014), High-frequency *Po*/*So* guided waves in the oceanic lithosphere: II—Heterogeneity and attenuation, *Geophys. J. Int.*, *199*, 614–630.

Mallick, S., and L. N. Frazer (1990), Po/So synthetics for a variety of oceanic models and their implications for the structure of the oceanic lithosphere, *Geophys. J. Int.*, *100*, 235–253.

Olugboji, T. M., S. Karato, and J. Park (2013), Structures of the oceanic lithosphere-asthenosphere boundary: Mineral-physics modeling and seismological signatures, *Geochem. Geophys. Geosyst.*, *14*, 880–901, doi:10.1002/ggge.20086.

Rubin, K. H., J. M. Sinton, J. Maclennan, and E. Hellebrand (2009), Magmatic filtering of mantle compositions at mid-ocean-ridge volcanoes, *Nat. Geosci.*, *2*, 321–328, doi:10.1038/ngeo504.

Saito, T. (2006), Synthesis of scalar-wave envelopes in two-dimensional weakly anisotropic random media by using the Markov approximation, *Geophys. J. Int.*, *165*, 501–515.

Sato, H., M. C. Fehler, and T. Maeda (2012), *Seismic Wave Propagation and Scattering in the Heterogeneous Earth*, 2nd ed., Springer, Heidelberg, Germany.

Schmerr, N. (2012), The Gutenberg discontinuity: Melt at the lithosphere-asthenosphere boundary, *Science*, *335*, 1480–1483, doi:10.1126/science.1215433.

Sereno, T. J., and J. A. Orcutt (1985), Synthesis of realistic oceanic P*n* wave-trains, *J. Geophys. Res.*, *90*, 12,755–12,776.

Sereno, T. J., and J. A. Orcutt (1987), Synthetic P*n* and S*n* phases and the frequency dependence of Q of oceanic lithosphere, *J. Geophys. Res.*, *92*, 3541–3566.

Shearer, P. M., and P. S. Earle (2004), The global short-period wavefield modelled with a Monte Carlo seismic phonon method, *Geophys. J. Int.*, *158*, 1103–1117.

Shito, A., D. Suetsugu, T. Furumura, H. Sugioka, and A. Ito (2013), Small-scale heterogeneities in the oceanic lithosphere inferred from guided waves, *Geophys. Res. Lett.*, *40*, 1708–1712, doi:10.1002/grl.50330.

Shito, A., D. Suetsugu, and T. Furumura (2015), Evolution of the oceanic lithosphere inferred from Po/So waves traveling in the Philippine Sea Plate, *J. Geophys. Res. Solid Earth*, *120*, 5238–5248, doi:10.1002/2014JB011814.

Sun, D., M. S. Miller, N. P. Agostinetti, P. D. Asimow, and D. Li (2014), High frequency seismic waves and slab structures beneath Italy, *Earth Planet. Sci. Lett.*, *391*, 212–223.

Tommasi, A., and A. Ishikawa (2014), Microstructures, composition, and seismic properties of the Ontong Java Plateau mantle root, *Geochem. Geophys. Geosyst.*, *15*, 4547–4569, doi:10.1002/2014GC005452.